The optical variability of radio-loud quasars

Minfeng Gu
Shanghai Astronomical Observatory

in collaboration with Yanli Ai (YNAO/NAOC)

2012.06.21
Black Hole Universe 2012, Bamberg

Outlines

- Introduction & motivation
- The optical variability & spectral index – brightness relation
- Summary

Radio-loud quasars

- Radio loudness: $R \equiv L_{\nu 5\ \mathrm{GHz}}/L_{\nu 4400}$,

  R>10 radio-loud; <1 radio-quiet; 1<R<10 radio intermediate (Kellermann et al. 1994)
- Radio luminosity: $P_{6\ \mathrm{cm}} \approx 10^{25}\ \mathrm{W\,Hz^{-1}\,sr^{-1}}$ (Miller et la. 1990)
- Radio dichotomy: 90% radio quiet; 10% radio loud (Kellermann et al. 1989, Ivezic et al. 2002, 2004)
- Flat-spectrum radio quasars (FSRQs); Steep-spectrum radio quasars (SSRQs)

  (α < 0.5 flat; >0.5 steep; $f_\nu \propto \nu^{-\alpha}$)

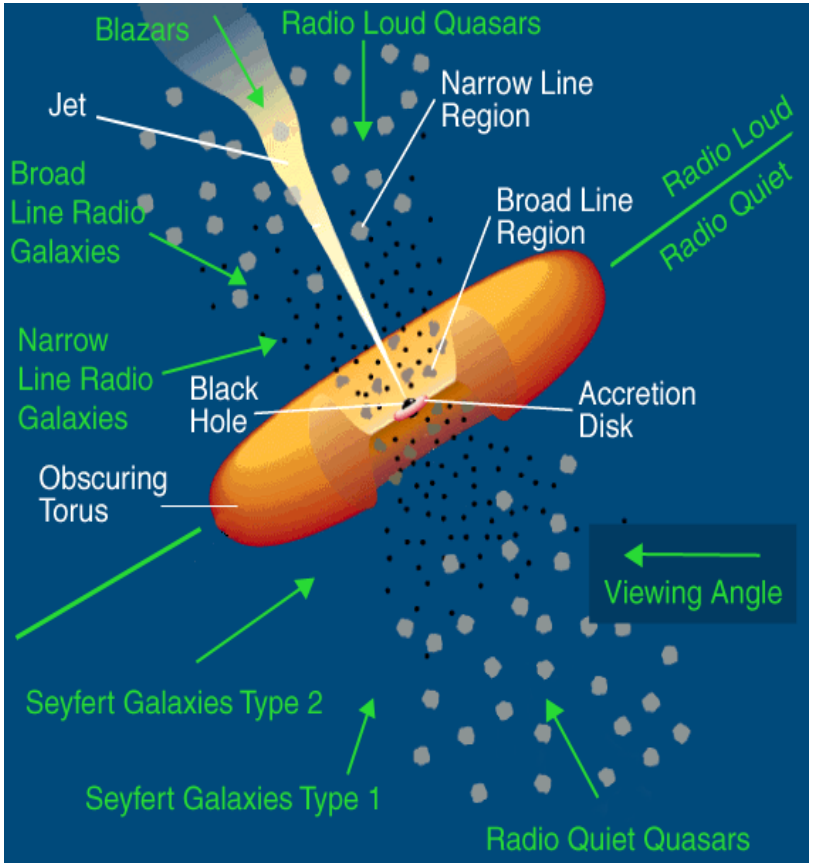

Urry & Padovani (1995)

- Blazars: BL Lacs and Flat-spectrum radio quasars (FSRQs)
- Synchrotron + Inverse Compton (e.g. SSC, EC)
- Jet dominated
- Voilent variability

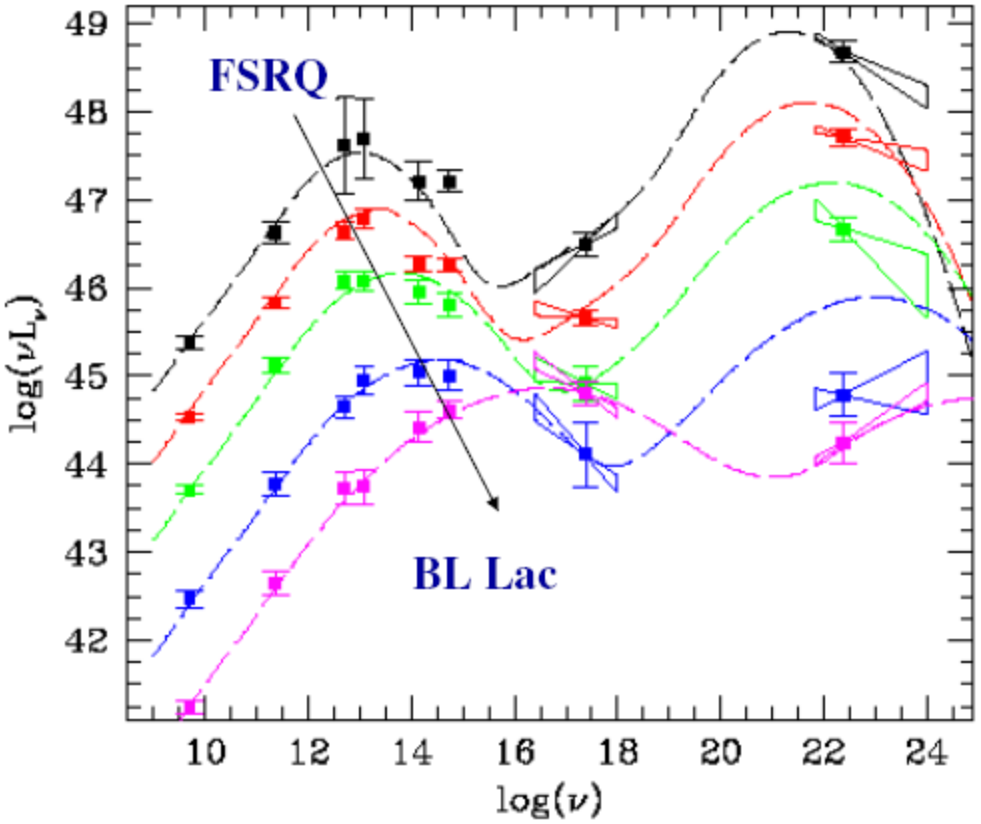

(Fossati et al. 1998)

Emission in FSRQs

- Jet emission is thought to be dominated due to the jet axis closer to the line of sight producing Doppler boosting in jet emission.
- However, thermal emission can be dominant in some FSRQs, e.g. 67/185 thermal-dominated sources in Chen, Gu & Cao (2009), see also Gu et al. (2006)

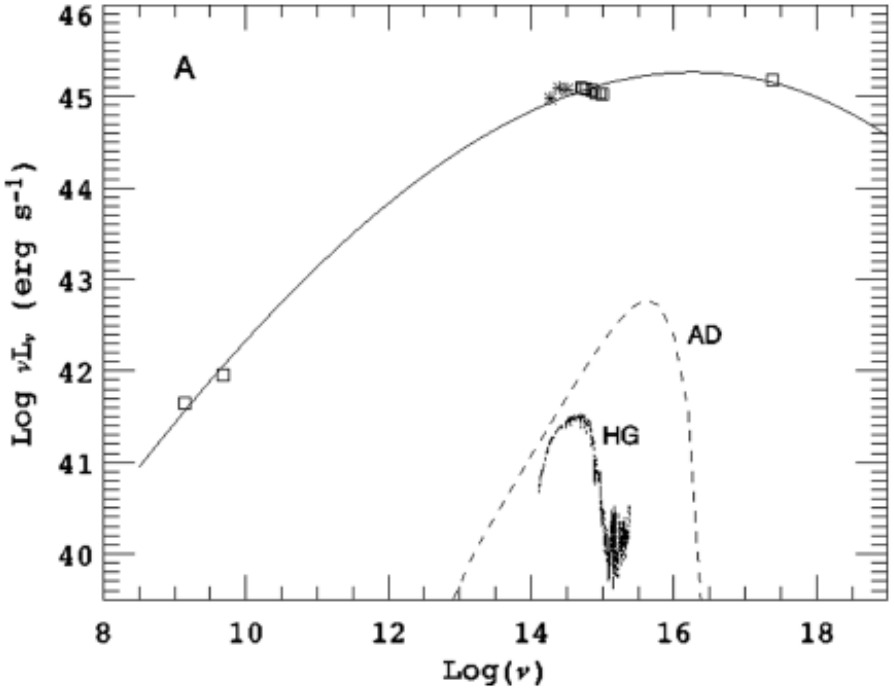

Thermal & non-thermal emission

accretion disk & jet

- L_{BLR} & $L_{continuum}$ relation: Mg II – $L_{3000Å}$; Hβ - $L_{5100Å}$
- FSRQs may deviate from the relations of radio quiet AGNs, but not all.

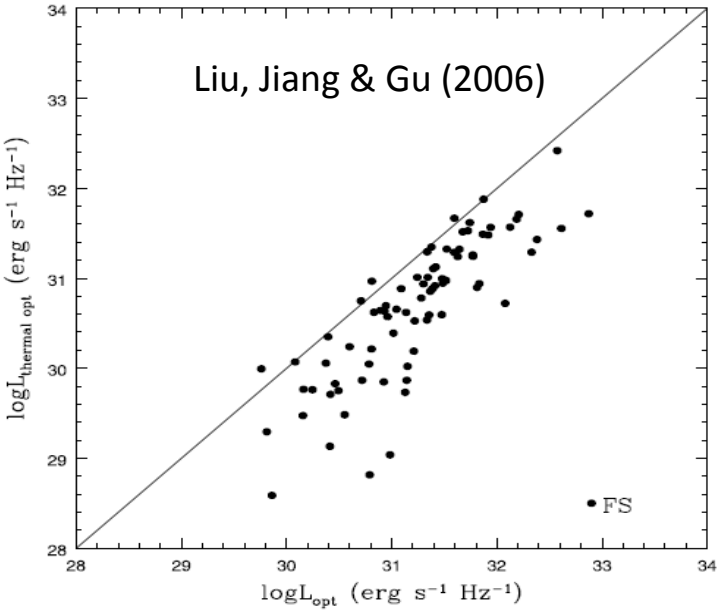

FIG. 4.—Thermal optical luminosity estimated using eq. (6) and the measured optical luminosity for FSRQs. The solid line is the equivalent line. [*See*

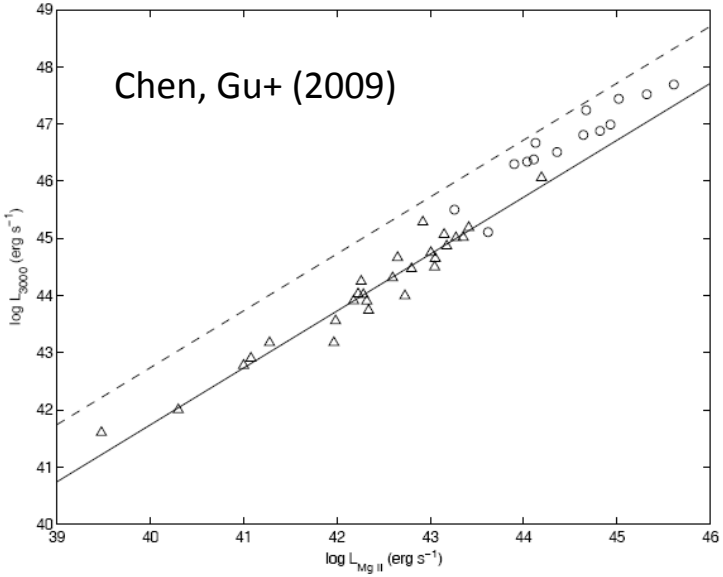

Fig. 2 Luminosity at 3000 Å versus broad Mg II luminosity. The open circles are our FSRQs, while open triangles represent the radio-quiet AGNs in Kong et al. (2006). The solid line is the OLS bisector linear fit to radio-quiet AGNs in Kong et al. (2006), $\lambda L_{\lambda 3000\,\mathring{\rm A}} = 78.5\, L^{0.996}_{\rm Mg\ II}$ (see Eq. (7)). The dashed line represents the deviation from the solid line by one order of magnitude in $\lambda L_{\lambda 3000\,\mathring{\rm A}}$, which is used to indicate the deviation of our FSRQs from the relation for radio-quiet AGNs.

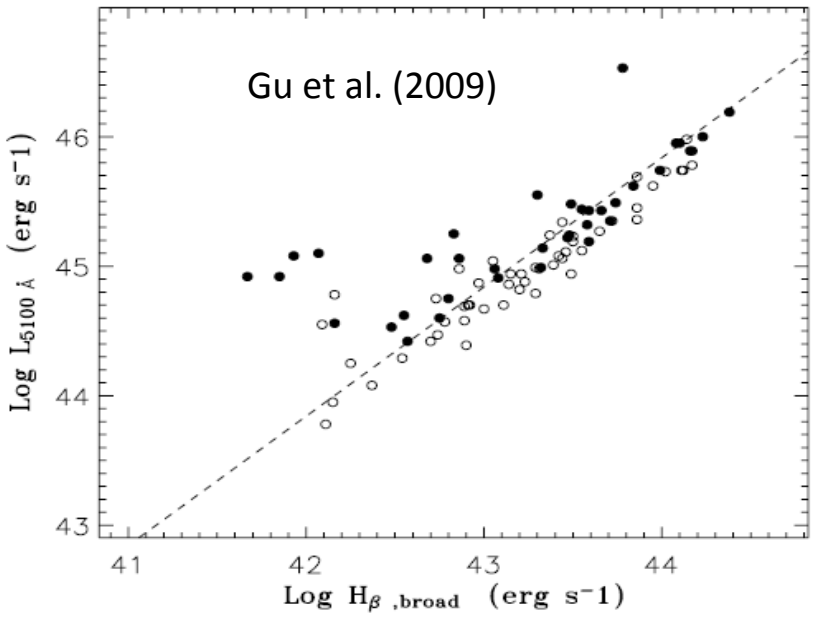

Figure 2. The luminosity at 5100 Å versus the broad Hβ luminosity. The symbols are the same as in Fig. 1. The dashed line is the OLS bisector linear fit to Kaspi et al. (2000) radio-quiet AGN (see Liu et al. 2006).

PKS 1222+216: a TeV-detected FSRQ

- Hβ luminosity is practically constant while the continuum is highly variable (Farina et al. 2012).

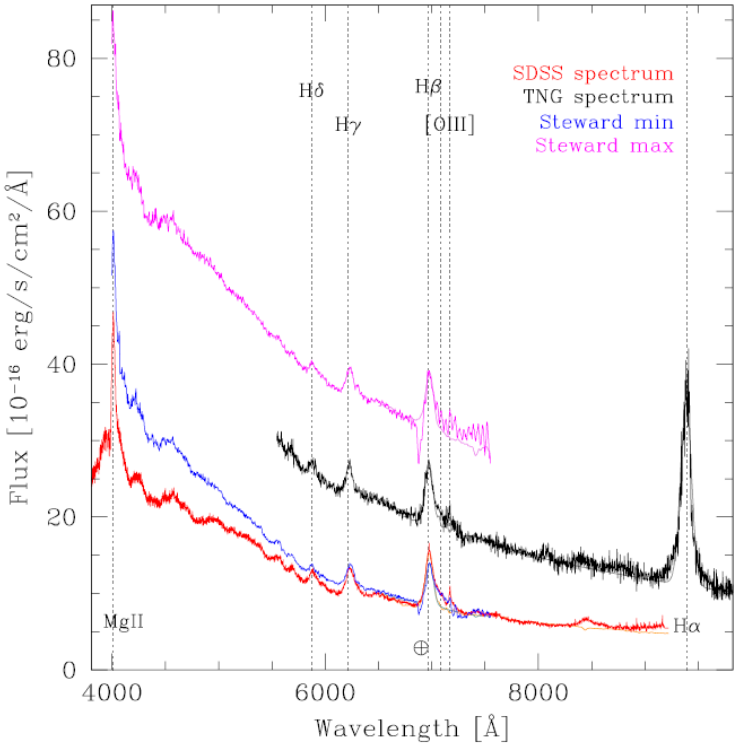

Figure 1. Dereddened spectra of PKS 1222+216 from: SDSS (red line), TNG (black solid line) and Steward observatory in correspondence of minimum (blue line) and maximum (magenta line) optical activity. The results of our fitting procedure on Hβ and Hα broad line are plotted in light colors. Most prominent emission lines are marked with grey dotted vertical lines and the ⊕ symbol highlights the strong telluric absorption that affects the Steward observatory spectra at ∼ 6900Å. A colour version of this figure is available in the electronic edition of MNRAS.

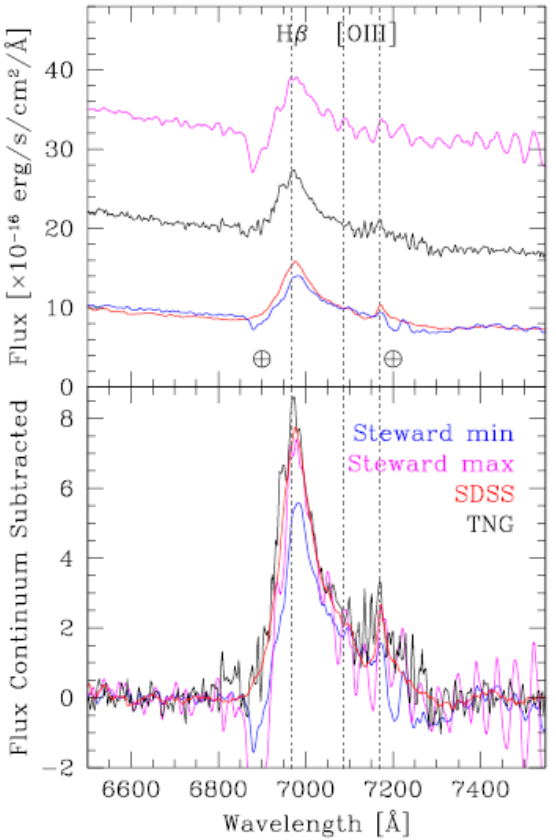

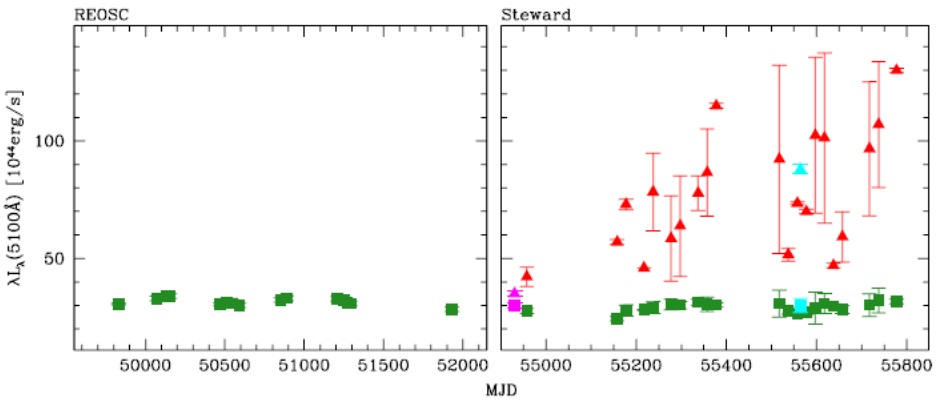

Figure 2. Luminosity of the measured continuum (triangle) and of the thermal component (squares) as a function of time. In the *Left Panel* we present data deduced from the REOSC photometry assuming an average spectral index $\alpha = -0.44$ (see §3). These correspond to a status of minimum optical activity of the FSRQ. The *Right Panel* shows the measures from Steward observatory spectra (red filled triangle: continuum measured at 5100 Å, and green filled squares: thermal continuum calculated from Hβ luminosity). Cyan points are from TNG spectrum, and the magenta ones from SDSS (for the sake of clarity, this latter, observed the MJD(SDSS)=54479, is shifted at MJD=54925). Steward observatory and REOSC data are resampled in 20 days bins, and the plotted errors are the standard deviations. Uncertainties on the SDSS and TNG thermal continuum luminosities are the rms of the relation presented in §3.

The thermal emission indicated from variability: color & brightness in FSRQs

- The bluer-when-brighter trend is commonly observed in blazars (Ghisellini et al. 1997; Fan et al. 1998b; Massaro et al. 1998; Ghosh et al. 2000; Clements & Carini 2001; Raiteri et al. 2001; Villata et al. 2002).
- But, opposite examples were also found, (e.g. 3C 454.3 Gu et al. 2006; Rani et al. 2010): FSRQs commonly show redder-when-brighter trend.
- Other examples: PKS 0736+017 (Clements et al. 2003; Ramírez et al. 2004), 3C 446 (Miller 1981), PKS 1622-297 & CTA 102 (Osterman Meyer et al. 2008,2009).

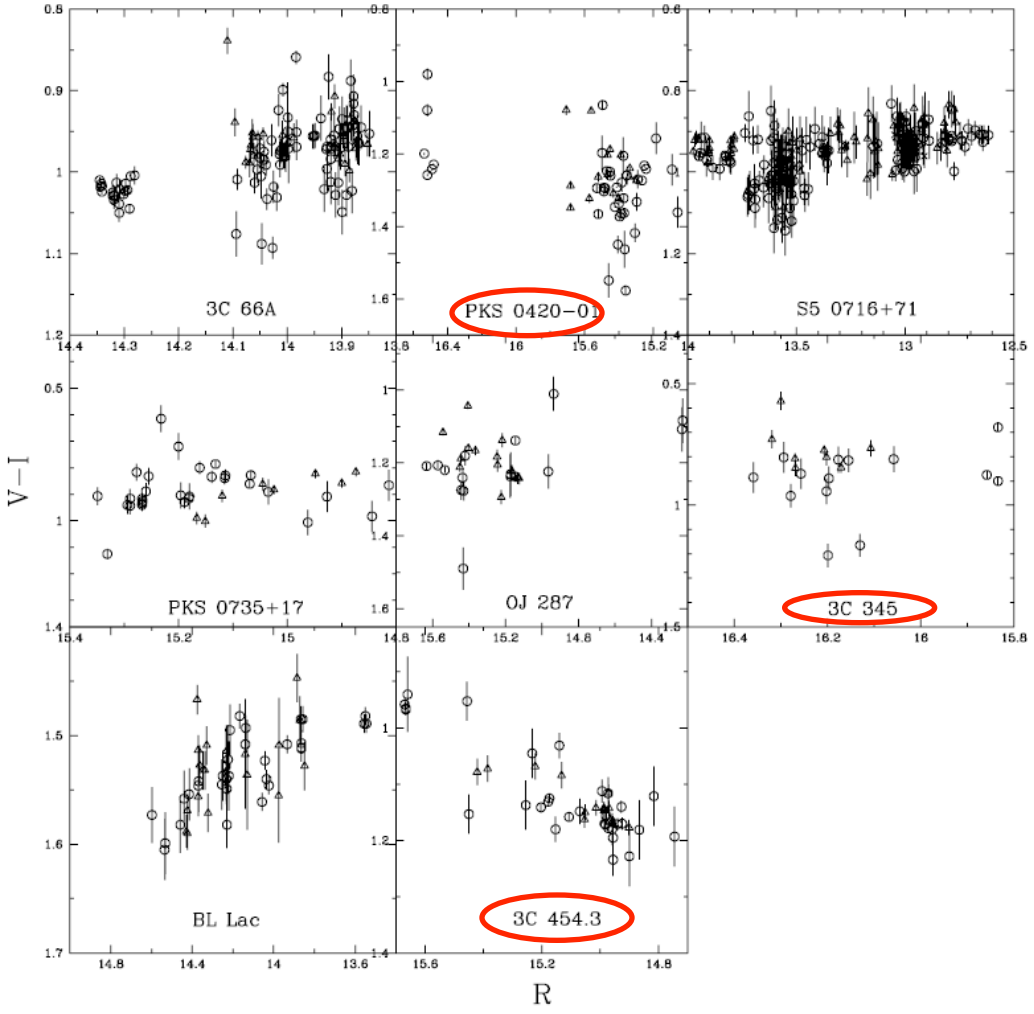

Gu et al. (2006)

Scenario for redder-when-brighter trend

- Competition of Big Blue Bump & Synchrotron (e.g. Gu et al. 2006)
- UV excess in 3C 454.3 during lower flux states (Raiteri et al. 2007)
- Thermal blue bump in 3C 345 (Webb et al. 1994)
- Emerging of accretion disk emission when synchrotron emission drops in NLS1s PMN J0948+0022 (Abdo et al. 2009)

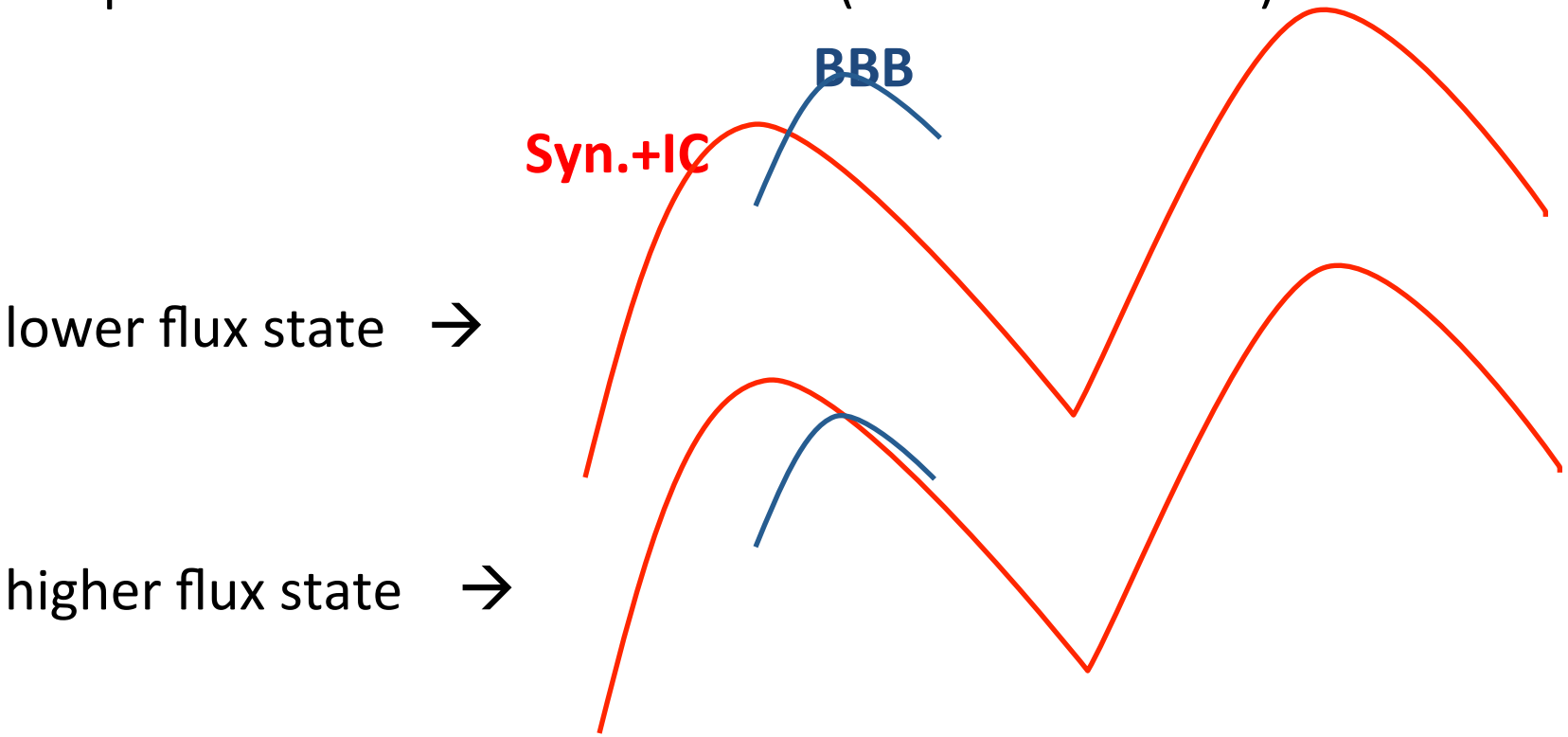

Emission in SSRQs

- SSRQs are usually lobe-dominated radio quasars, with radio lobe emission dominate over the radio core emission.
- Their jets are viewed at larger angles than blazars. Therefore, the beaming effects from jets should not be severe (see e.g. Liu et al. 2006), and the jet emission is not expected to dominate at optical bands (e.g. Gu & Ai 2011a).

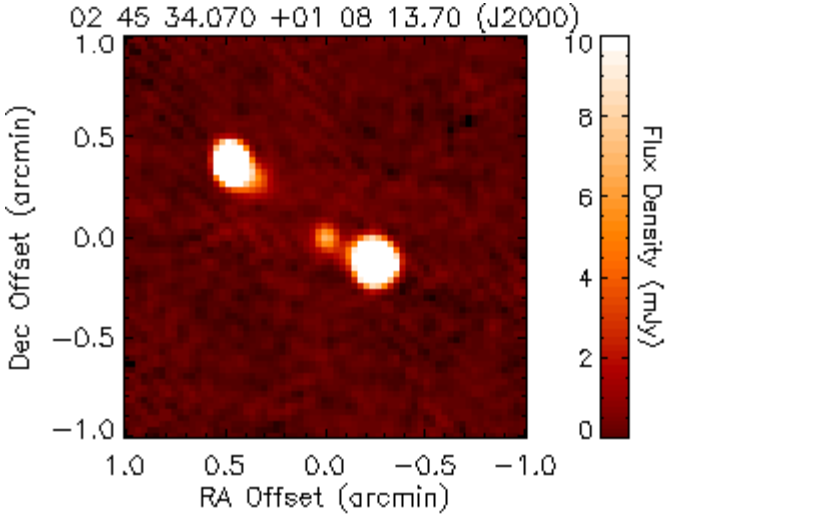

- Cleary et al. (2007): 3CRR galaxies and quasars at z: 0.4 – 1.2 with the spitzer IRS and MIPS observations
- Quasars are more luminous in the mid-infrared than galaxies because of a combination of synchrotron emission in quasars and extinction in galaxies

- Antonucci et al. (1990): mm observations – no evidence of synchrotron emission in IR band.

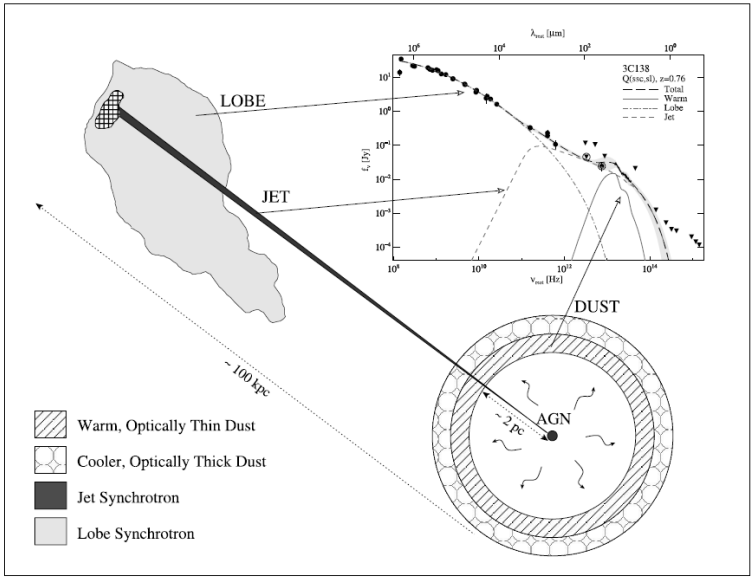

FIG. 3.—This cartoon indicates the physical origin of the broadband spectral components used to fit the SEDs, using the SED of the quasar 3C 138 as an example (see Fig. 13). The drawing is not to scale: the dust shell has been drawn $\approx 10^4$ times its correct size relative to the extent of the jet.

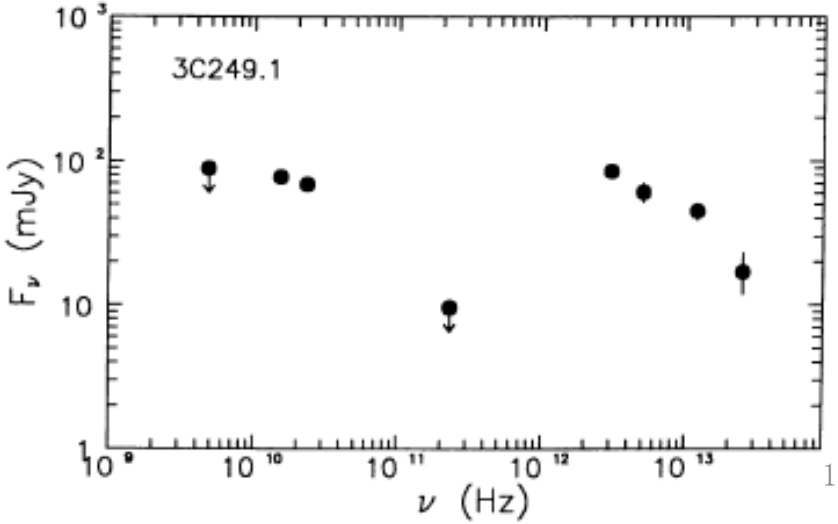

Motivations

- What's the general color behavior in FSRQs ?

- The optical variations of SSRQs are largely unknown, and there are only few explorations on variations in SSRQs (e.g. Stalin et al. 2004, 2005), as well as their color behavior.
- The mechanism of optical/UV emission in SSRQs.

A sample of radio-loud quasars from SDSS stripe 82 region (Gu & Ai 2011a,b)

- Quasars sample:

  SDSS DR7 quasars catalogue

- Optical multi-epoch monitoring:

  SDSS stripe 82 region

- Radio emitters at two radio frequencies:

  FIRST, NVSS, GB6 and PMN

- Radio spectral index:

  $\alpha < 0.5$ ($f_\nu \propto \nu^{-\alpha}$) – flat; >0.5 - steep

SDSS Stripe 82 region

- The Equatorial Stripe (ra > 310° or ra < 59°; -1°.25 > dec < 1°.25), about 270 deg^2
- Repeatedly scanned during the SDSS-I phase (2000 - 2005) under generally photometric conditions (calibrations - Lupton et al. 2002)
- Three 3-month campaigns in three successive years in 2005 – 2007, known as SDSS Supernova Survey (SN survey, Frieman et al. 2008)
- Mostly during the fall (September to December)

Stripe 82

- Temporal coverage (left)
- Separation in days between consecutive observations

Bhatti et al. (2010)

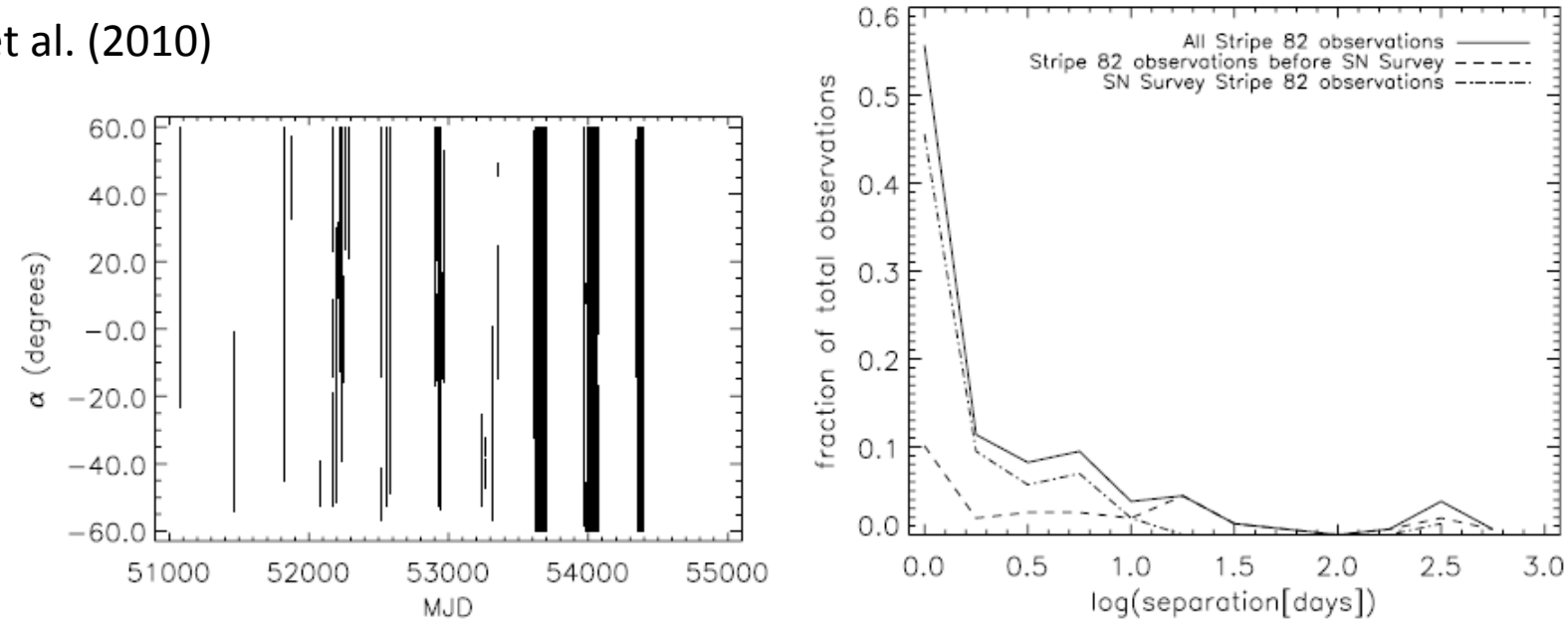

Figure 1. Left: Stripe 82 run temporal coverage vs. right ascension. The dense clusters at the right are the observation runs associated with the Supernova Survey. Note the large gaps between successive years of coverage of the Stripe. Right: histogram of the separation in days between consecutive observations of Stripe 82. The bins are 0.25 dex wide. The solid line represents all observations of the Stripe; the dashed line represents observations of the Stripe before the SN Survey; the dot-dashed line represents observations of the Stripe carried out during the SN Survey. The high relative cadence of the SN Survey observations is apparent.

Radio spectrum

- Quasars in stripe 82 region from SDSS DR7 quasars catalogue (Schneider et al. 2010)
- SDSS – FIRST within 2”; PMN, GB6 within 1’
- GB6, PMN – FIRST: single or multiple FIRST component within 1’
- FIRST – PMN, GB6 spectral index :

  37 sources - 5 SSRQs, 32 FSRQs (single)

  29 sources - 14 SSRQs, 15 FSRQs (multiple)

------66----------19----------47----------

- FIRST: Faint Images of the Radio Sky at Twenty Centimeters; 1.4-GHz; beam size 5”.4; VLA (Becker et al. 1995)
- GB6: Green Bank 6-cm (GB6) survey; 4.85 GHz; 3’.5 resolution (Gregory et al. 1996)
- PMN: Parkes-MIT-NRAO (PMN) radio continuum surveys; 4.85 GHz; beam FWHM 5’; dec. -87°- +10° (Griffith et al. 1995)

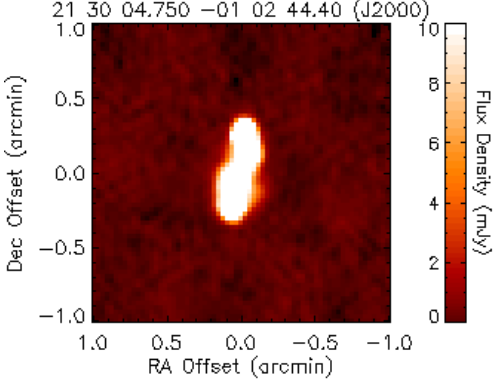

67 x 67 pixels extracted from FIRST image 21315−010
Brightest pixel is 116.94 mJy/beam at
X, Y = 35, 43 pixels
RA, Dec = 21 30 04.599 −01 02 28.72 (J2000)
RMS noise 0.203 mJy

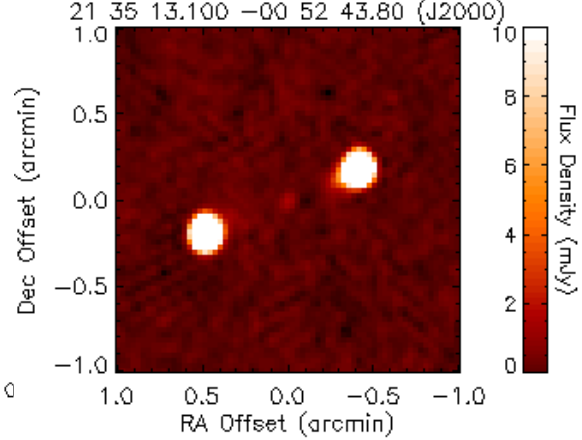

67 x 67 pixels extracted from FIRST image 21345−01
Brightest pixel is 167.33 mJy/beam at

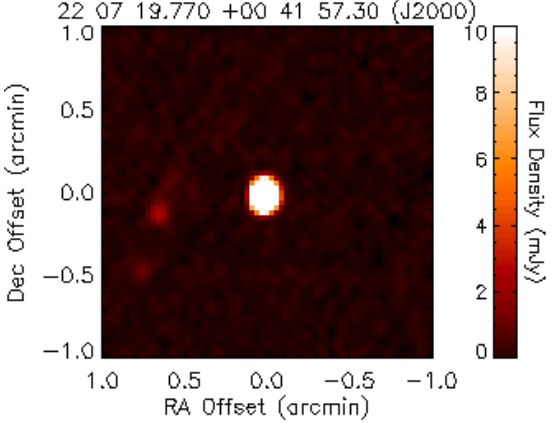

67 x 67 pixels extracted from FIRST image 22075+00390Z
Brightest pixel is 123.84 mJy/beam at
X, Y = 33, 33 pixels
RA, Dec = 22 07 19.853 +00 41 56.40 (J2000)

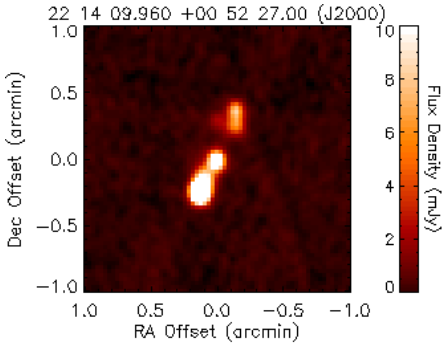

67 x 67 pixels extracted from FIRST image 22135+01050Z
Brightest pixel is 45.22 mJy/beam at
X, Y = 30, 26 pixels
RA, Dec = 22 14 10.445 +00 52 13.18 (J2000)

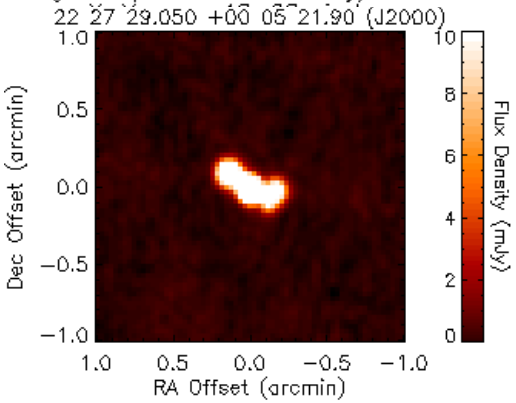

67 x 67 pixels extracted from FIRST image 22285+00130Z
Brightest pixel is 82.52 mJy/beam at

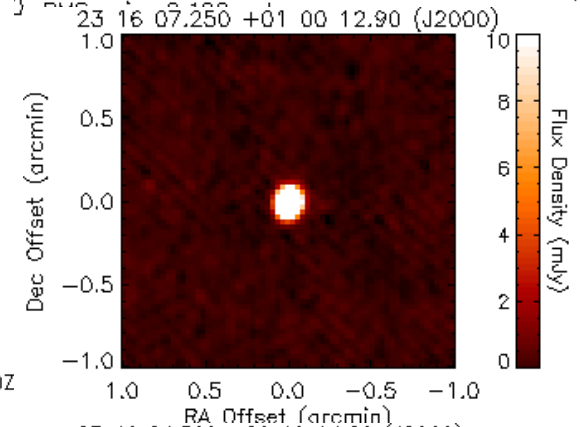

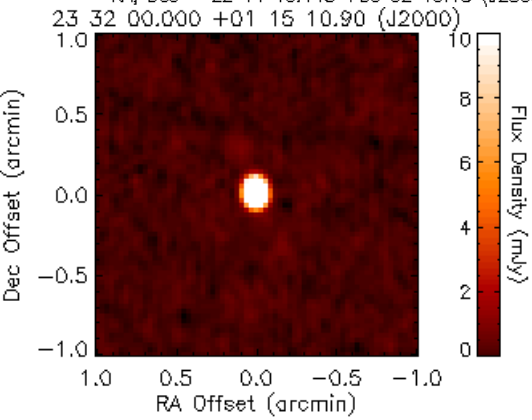

67 x 67 pixels extracted from FIRST image 23315+(
Brightest pixel is 80.65 mJy/beam at
X, Y = 34, 35 pixels
RA, Dec = 23 32 00.007 +01 15 11.99 (J200
RMS noise 0.154 mJy

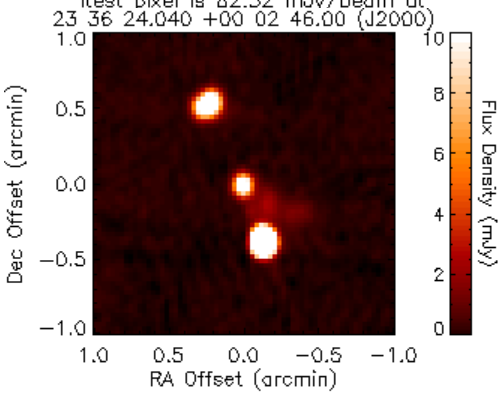

67 x 67 pixels extracted from FIRST image 23375+00130Z
Brightest pixel is 140.81 mJy/beam at
X, Y = 38, 21 pixels
RA, Dec = 23 36 23.573 +00 02 22.79 (J2000)
RMS noise 0.114 mJy

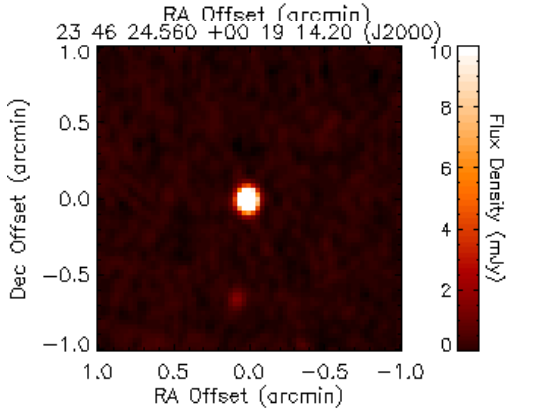

67 x 67 pixels extracted from FIRST image 23465+00130Z
Brightest pixel is 38.59 mJy/beam at
X, Y = 34, 34 pixels
RA, Dec = 23 46 24.533 +00 19 14.40 (J2000)
RMS noise 0.107 mJy

5/29 multi- NVSS counterparts within 1 arcmin: two examples

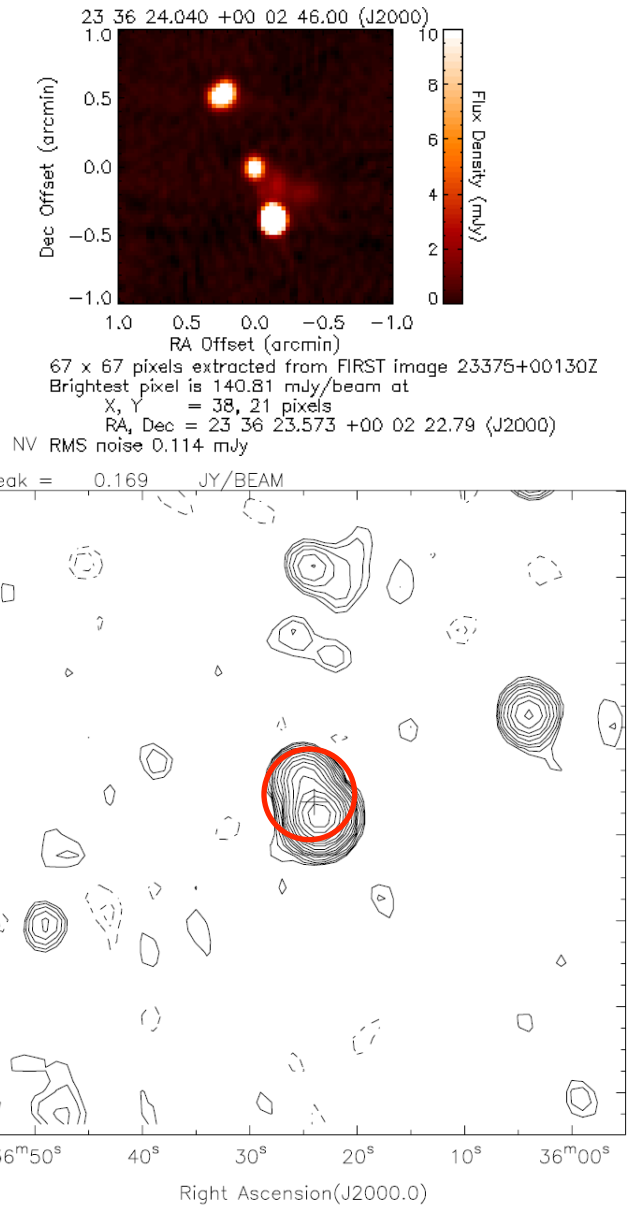

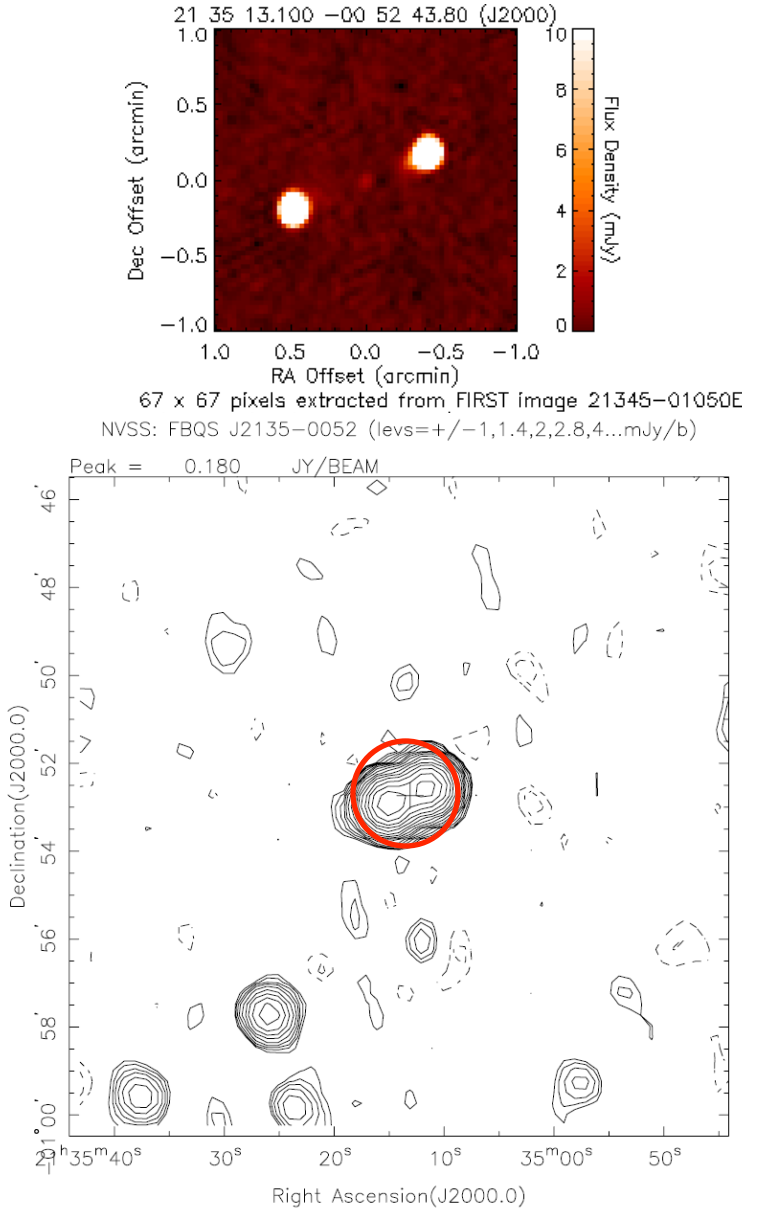

Sample parameters

- Shen et al. (2011): line measurements etc.
- M_{BH} from broad line luminosity and FWHM: Hβ (Vestergaard & Peterson 2006); Mg II and C IV (Kong et al. 2006)
- L_{BOL} from broad line luminosity (Celotti et al. 1997, Netzer 1990)

- z: 0.17<z<2.63 SSRQs
  0.34<z<2.7 FSRQs
- log R: 1.8,5.0
  1.55,4.48
- log M_{BH} : 8.29,10.08
  7.7,9.56
- log l: -2.35,0.52
  -2.03,0.57

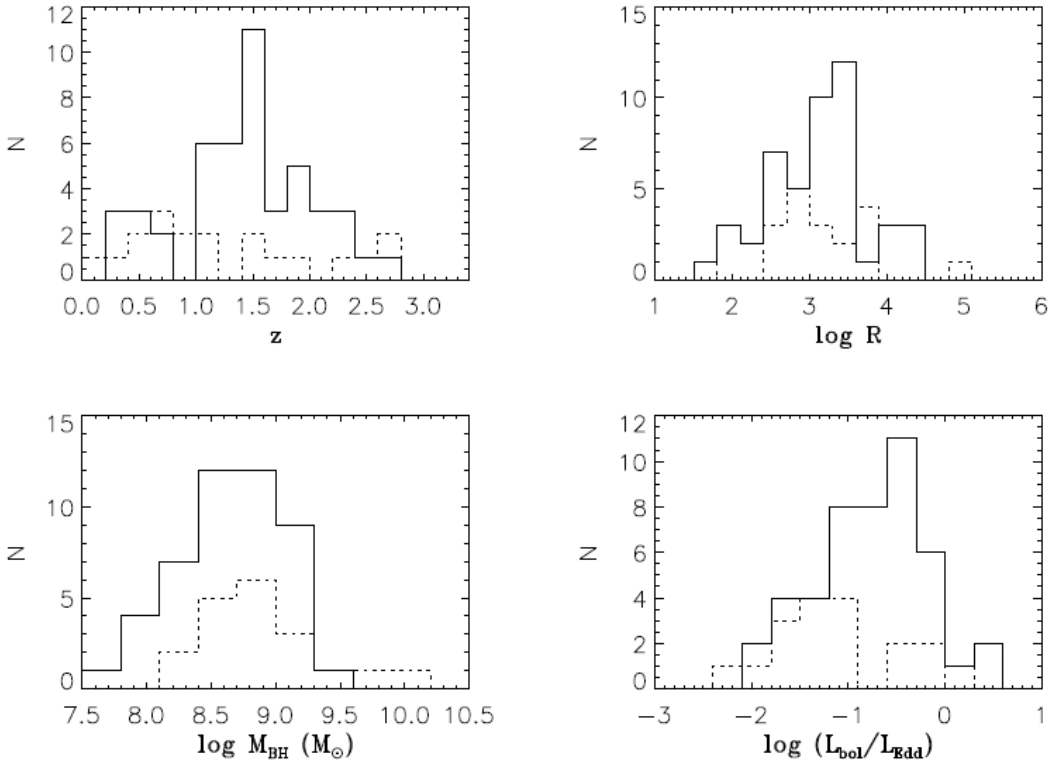

Fig. 1. The histogram of sample parameters: redshift (upper left), radio loudness (upper right), black hole mass (lower left), and the Eddington ratio (lower right). The dotted lines are for 19 SSRQs, and solid lines are for 47 FSRQs.

Stripe 82 region: photometry

- DR7 CAS : a total of 303 runs, covering any given piece of the approx. 270 deg^2 area approximately 80 times.
- Only about 1/4 of the Stripe 82 scans were obtained in photometric conditions, and the rest is non
  -photometric: CAS stripe82 database

- Select point sources classified in observational runs
- mag < magnitude limit=(ugriz: 22.0, 22.2, 22.2, 21.3, 20.5); exclude abnormal data, e.g. cloudy
- Power-law fit to ugriz flux --- get α_{opt}

Optical variability

- The variations in FSRQs are more pronounced.
- The variations at r band is 0.18 – 3.46 mag for FSRQs, which is much larger than that of radio quiet AGNs (e.g. NLS1s and BLS1s in Ai et al. 2010), but is typical for blazars. In contrast, it is 0.22 – 0.92 mag in SSRQs.

- Four FSRQs show Δr >1.0 mag:

  J001130.400+005751.80: Δr= 3.46 mag;

  J023105.597+000843.61: Δr= 1.02 mag;

  J025515.096+003740.55: Δr= 1.70 mag;

  J235936.817-003112.78: Δr= 1.20 mag.

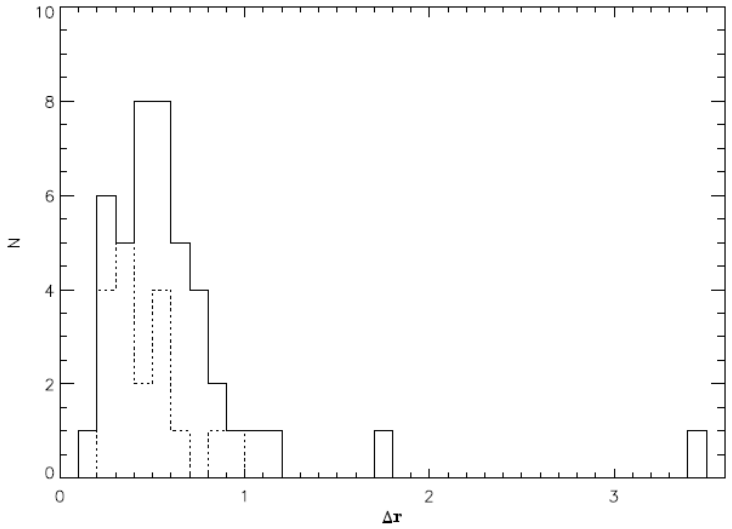

Fig. 8. The histogram of Δr for SSRQs and FSRQs in Gu & Ai (2011) and in this work. The dotted lines are for 18 SSRQs, and solid lines are for 44 FSRQs.

Spectral index & brightness

- FSRQs: 25/44 sources (~ 57%) have positive correlation indicating a BWB trend; SDSS J001130.400+005751.8 (z=1.4934) has a negative correlation at 99.99835% confidence level indicating a RWB trend.
- SSRQs: 8/18 sources (~ 44%) have a positive correlation.

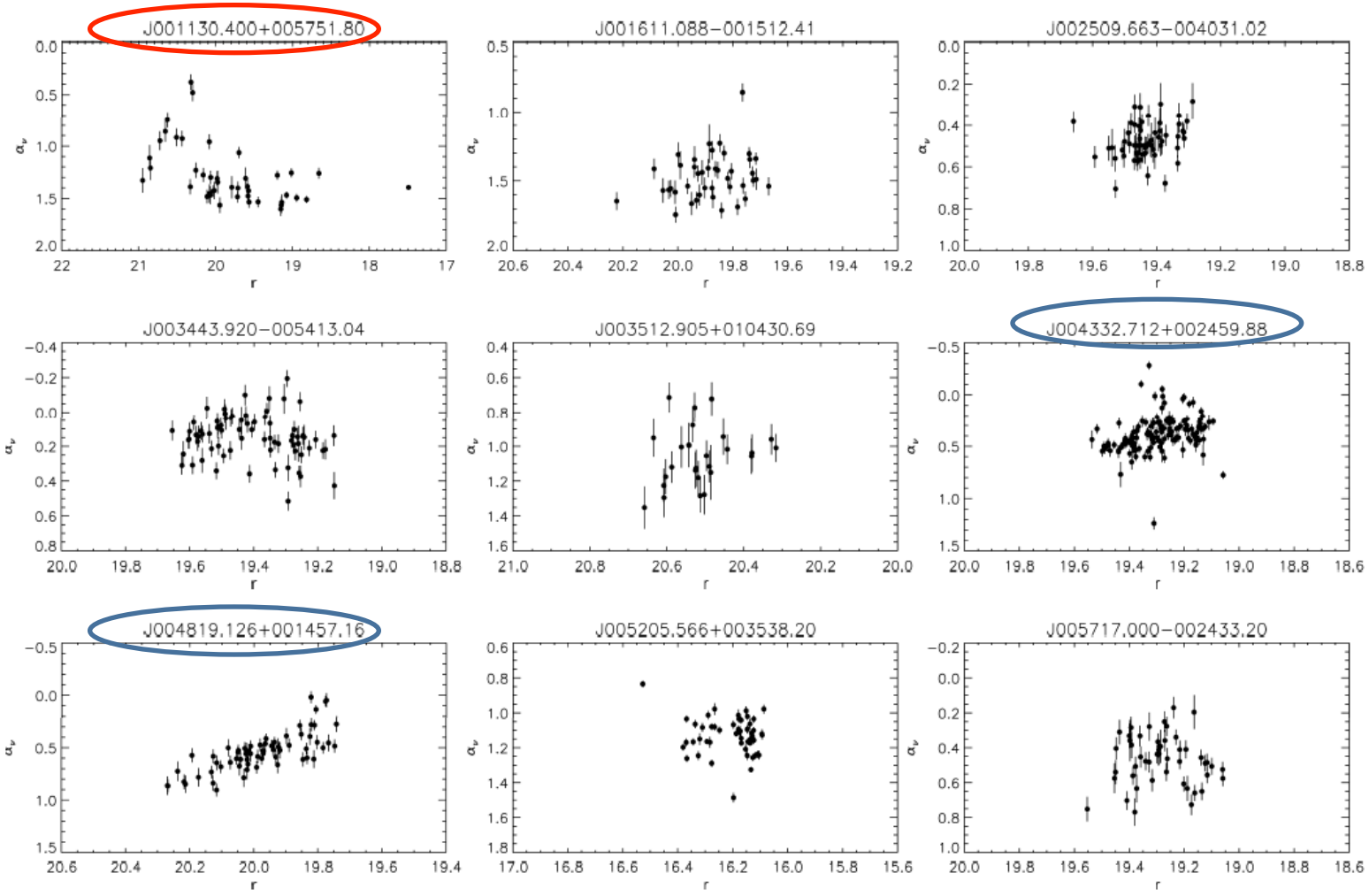

The only FSRQ with redder-when-brighter trend: SDSS J001130.400+005751.8 (z=1.4934) - light curve

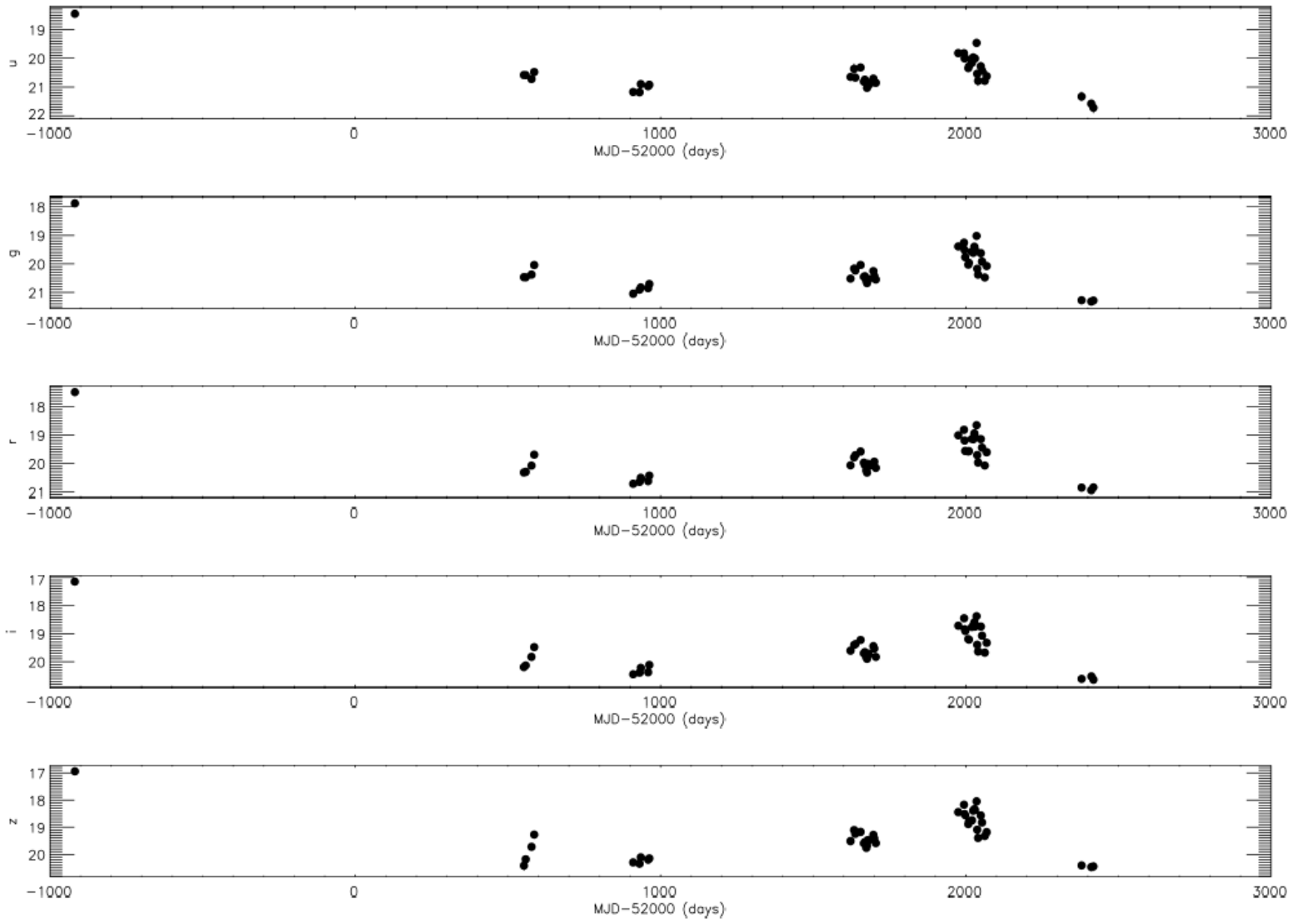

SDSS J001130.400+005751.8 variations: r band

- overall 3.46 mag

  17.49 mag: MJD=51081

  20.95 mag: MJD=54411
- 9 years coverage
- variations in each observational session

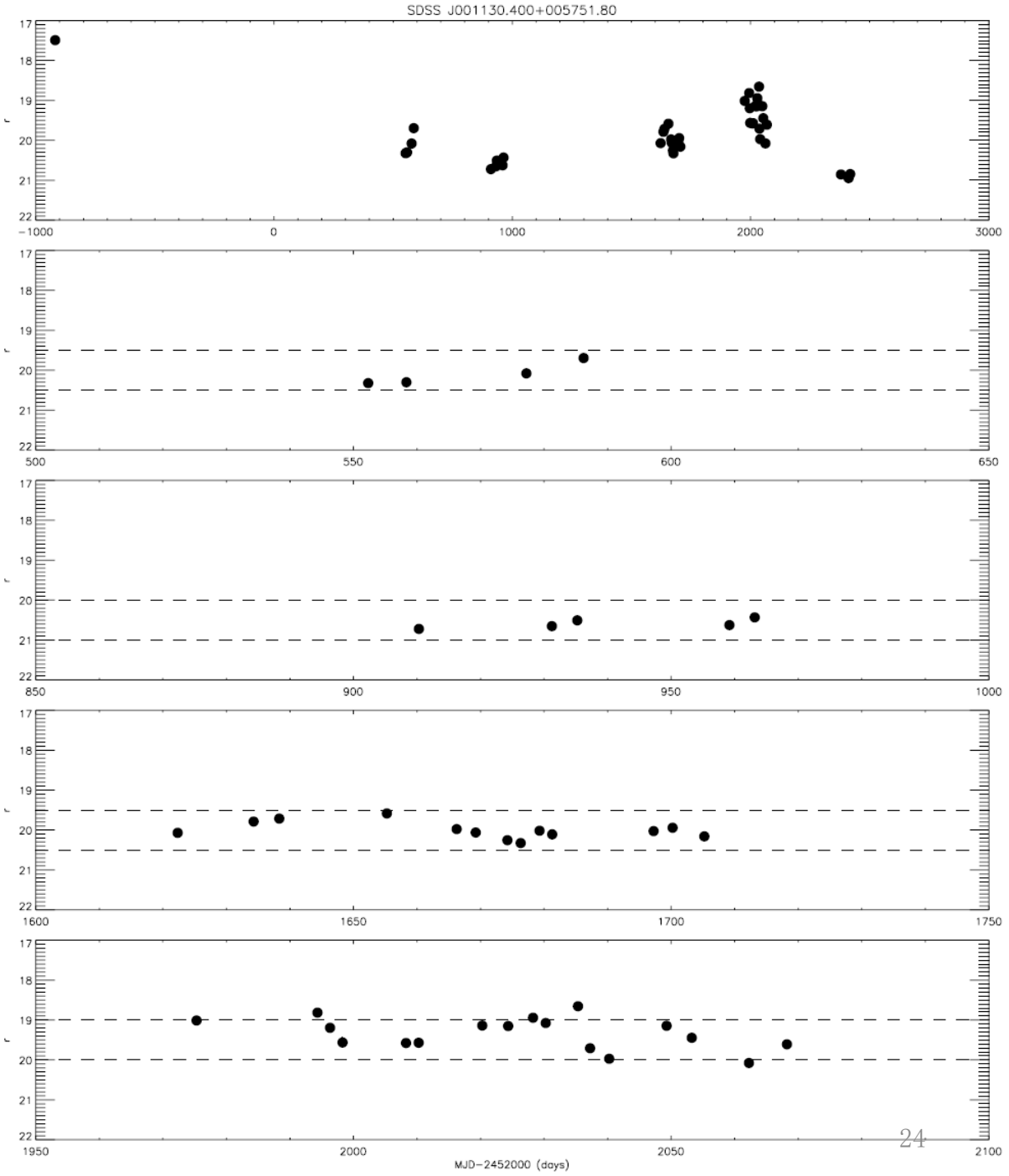

SDSS J001130.400+005751.8
NVSS & FIRST maps

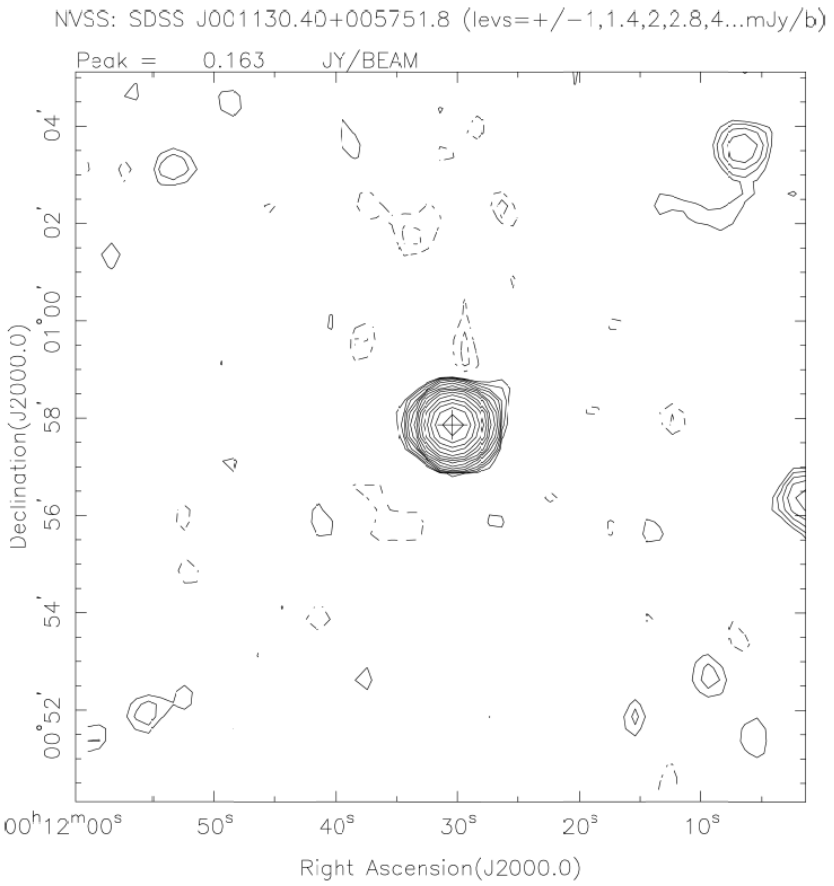

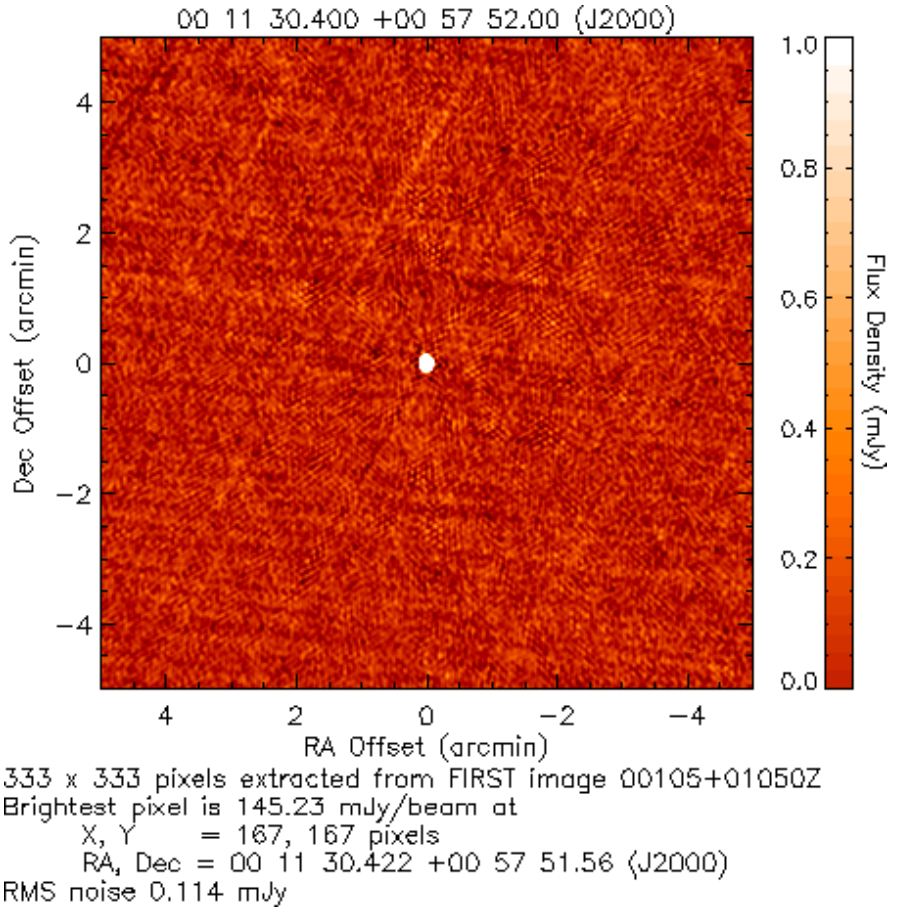

f_{FIRST}=156.07 mJy, f_{NVSS}=167.2 mJy

f_{PMN}=170 mJy (α= - 0.07 with f_{FIRST}), f_{GB6}=132.76 mJy (α=0.13 with f_{FIRST})

SDSS J001130.400+005751.8 VLBA map

- The fifth VLBA calibrator survey: VCS5 (Kovalev et al. 2007), 8.6 GHz, f_{int} = 90 mJy, $f_{unresolved}$ = 70 mJy

- VLA: $f_{8.4\ GHz}$ = 278.7 mJy (Healey et al. 2007); CRATES: Combined Radio All-Sky Targeted Eight GHz Survey

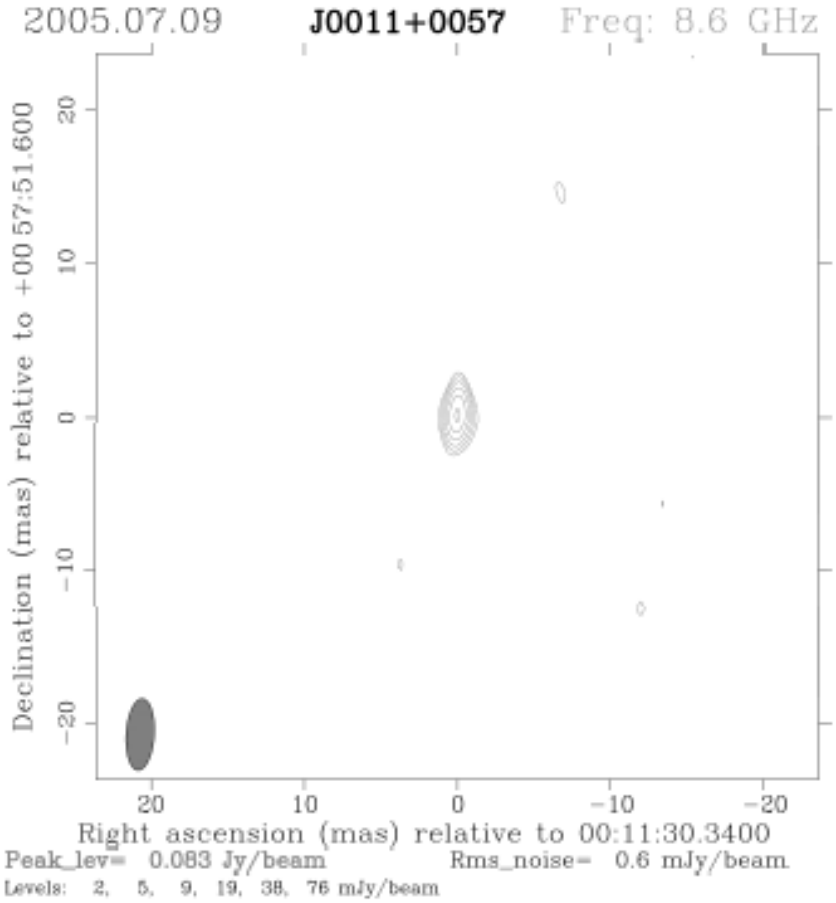

SDSS J001130.400+005751.8
SDSS spectra

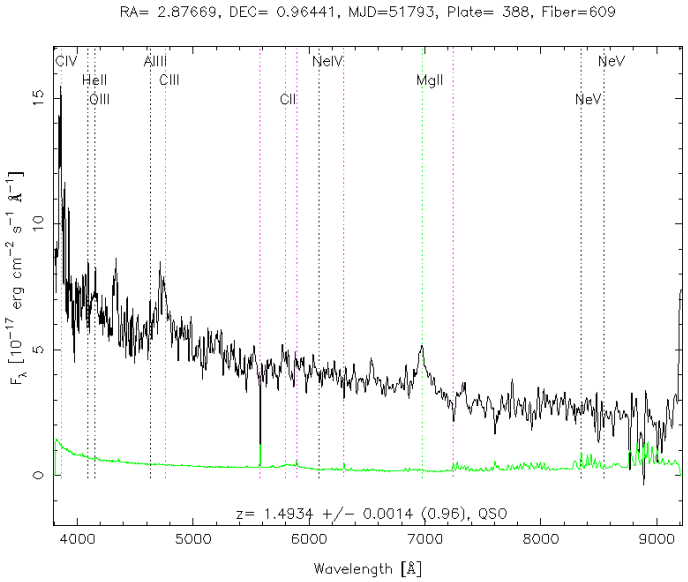

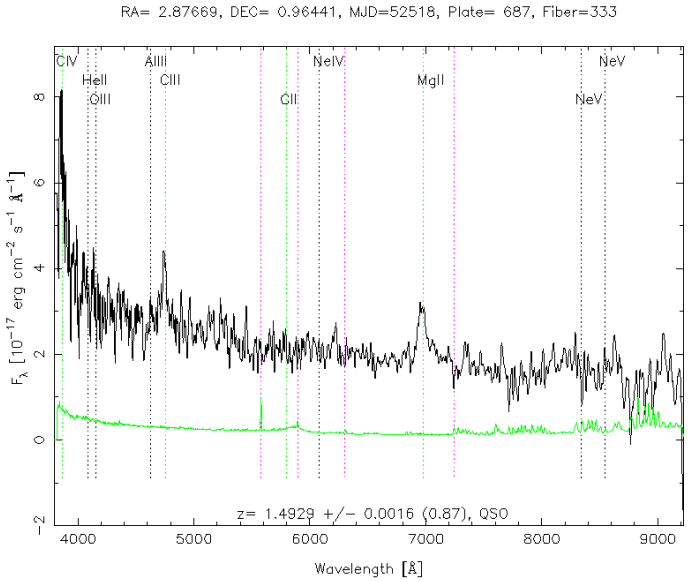

(upper, MJD=51793)

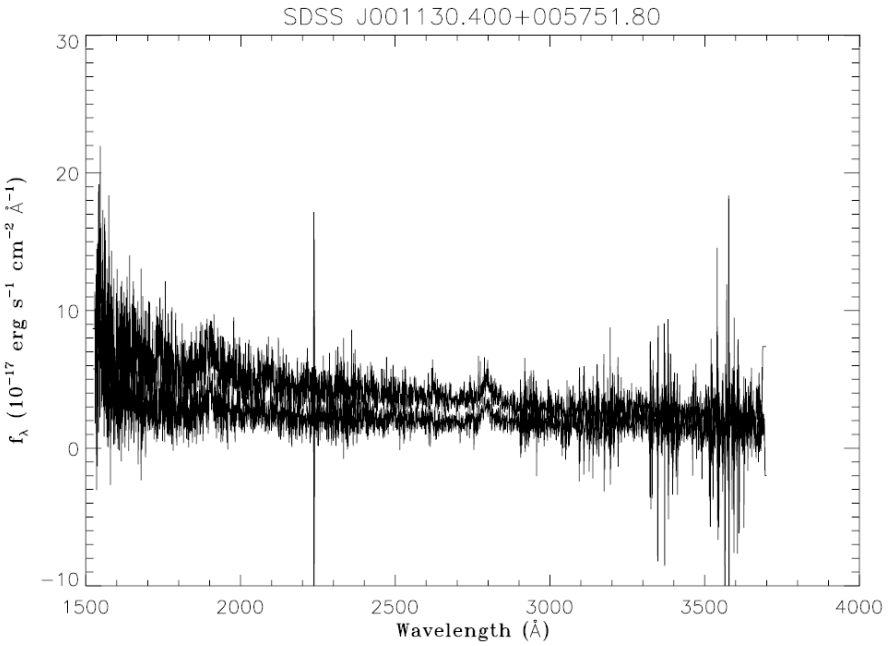

(lower, MJD=52518)

SDSS J001130.400+005751.8
The spectral data at lc and line-continuum plot

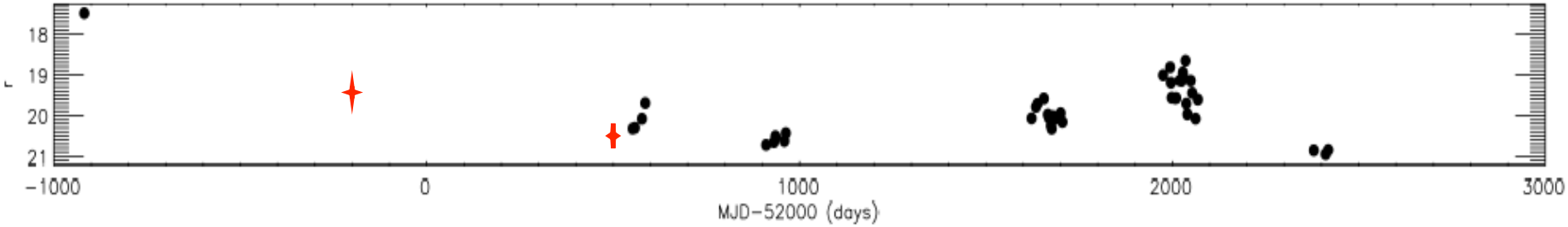

- SDSS spectra:

r ~ 19.64 mag @MJD=51793

r ~ 20.39 mag@MJD=52518

overall Δr on lc. (17.49,20.95)

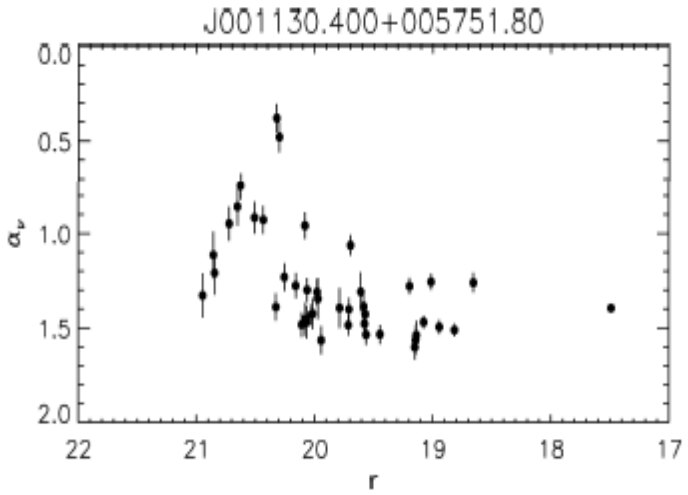

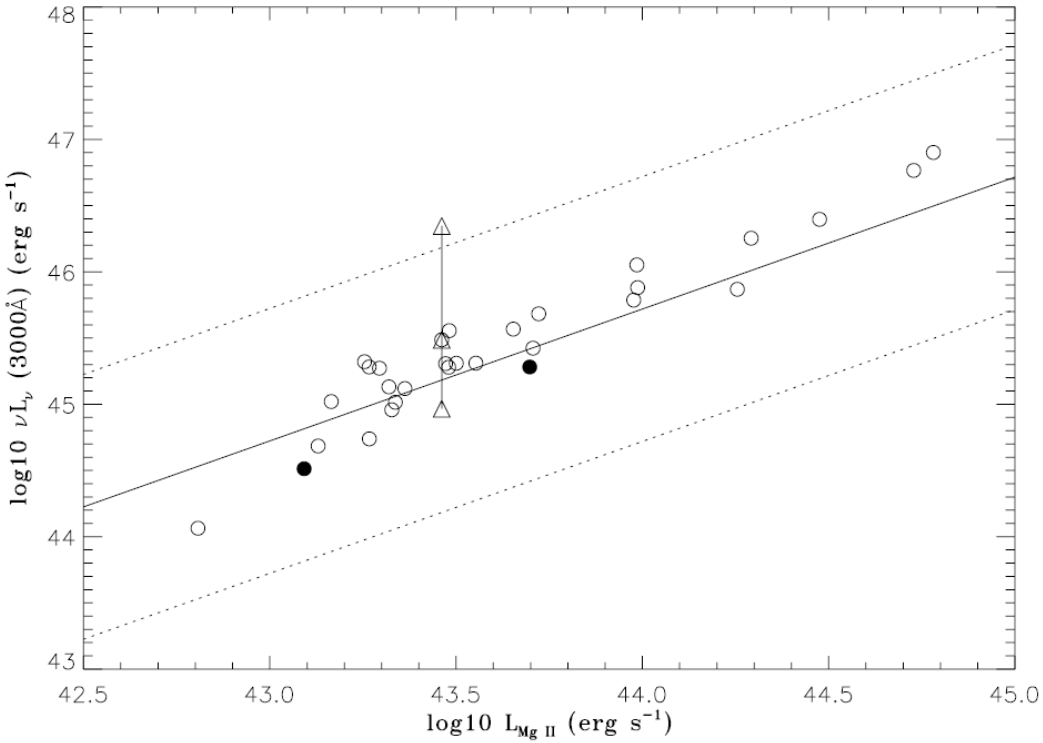

SDSS J001130.400+005751.8
Spectral Energy Distribution

- In the first Fermi Large Area Telescope AGNs catalogue (Abdo et al. 2010): photon index of 2.51±0.15; Low-synchrotron-peaked FSRQs, $<10^{14}$ Hz
- Classified as non-thermal dominated FSRQs (Chen, Gu & Cao 2009): log M_{BH}=8.36, log L_{bol}=46.28, log ν_p=14.95, log L_p =46.18
- SED from ASI Science Data Center blazar catalogue

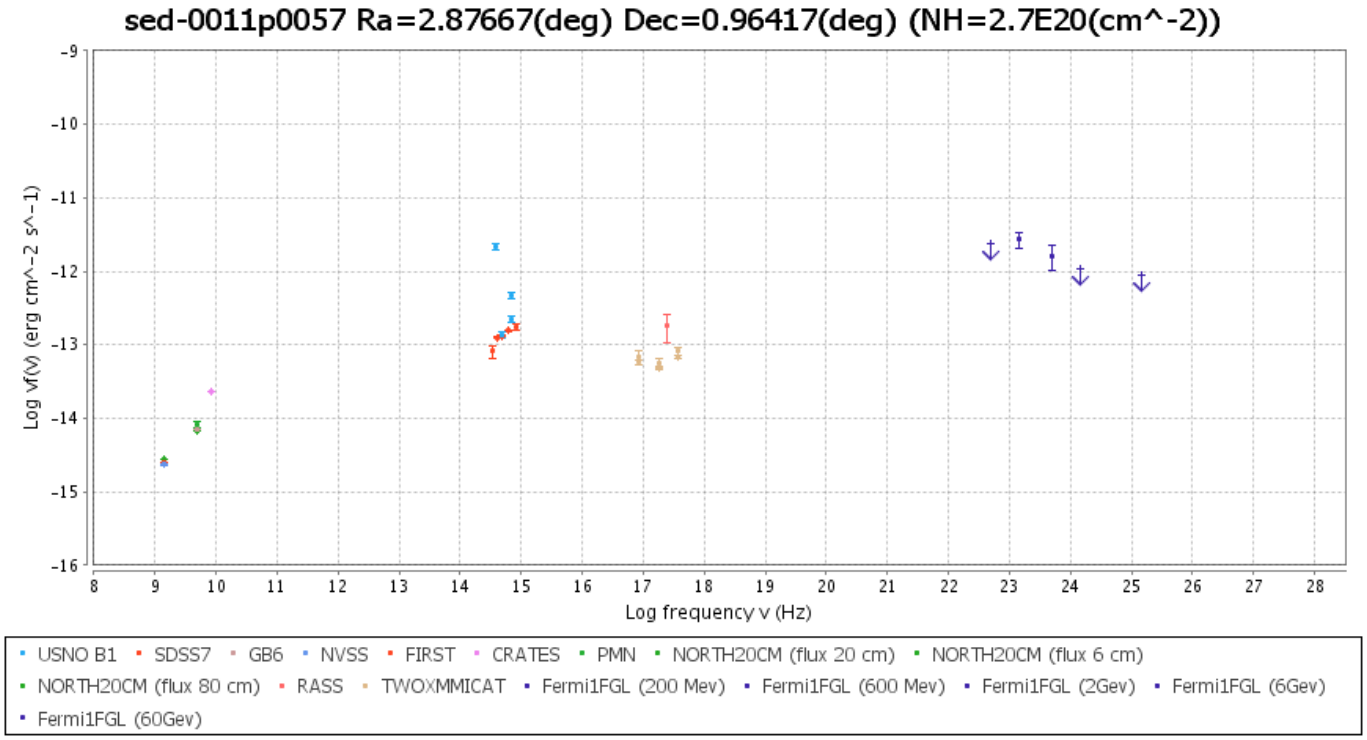

Mg II & continuum

- <log ($L_{3000Å}/L_{MgII}$)>=

  1.78±0.26 for SSRQs

  1.83±0.24 for FSRQs

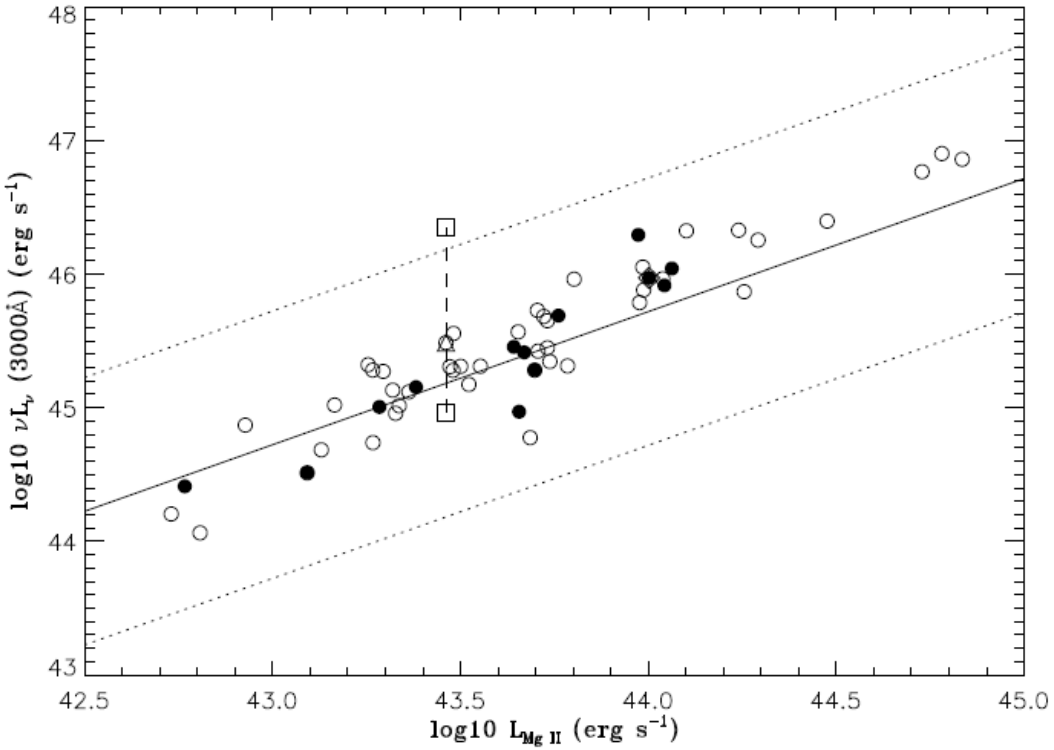

Fig. 6. The plot of broad Mg II line luminosity and continuum luminosity at 3000 Å for 13 SSRQs and 42 FSRQs. The diamond is for BALQ SDSS J024534.07+010813.7. The open triangle is SDSS J001130.40+005751.7. The solid line is the OLS bisector linear fit to radio-quiet AGNs in Kong et al. (2006), $\lambda L_{\lambda\ 3000Å} = 78.5\ L^{0.996}_{\mathrm{Mg\ II}}$.

- There is anti-correlation between Δr & Lbol/Ledd in SSRQs, which is similar to radio quiet AGNs, indicating the variability is likely from the thermal accretion disk emission.
- The broader Mg II line width with steeper radio spectral index implies a disk-like BLR geometry in our sample.

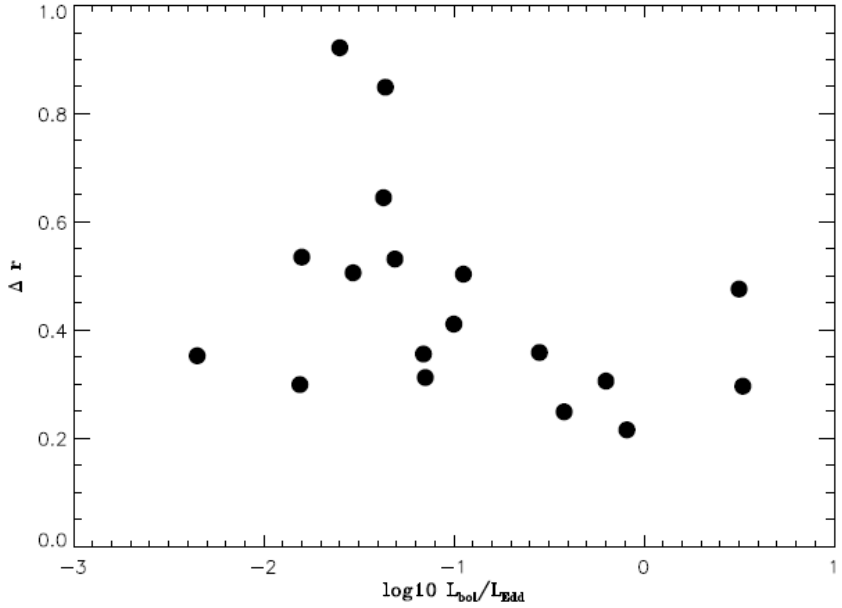

Fig. 7. The Eddington ratio versus the variability at r band Δr for SSRQs.

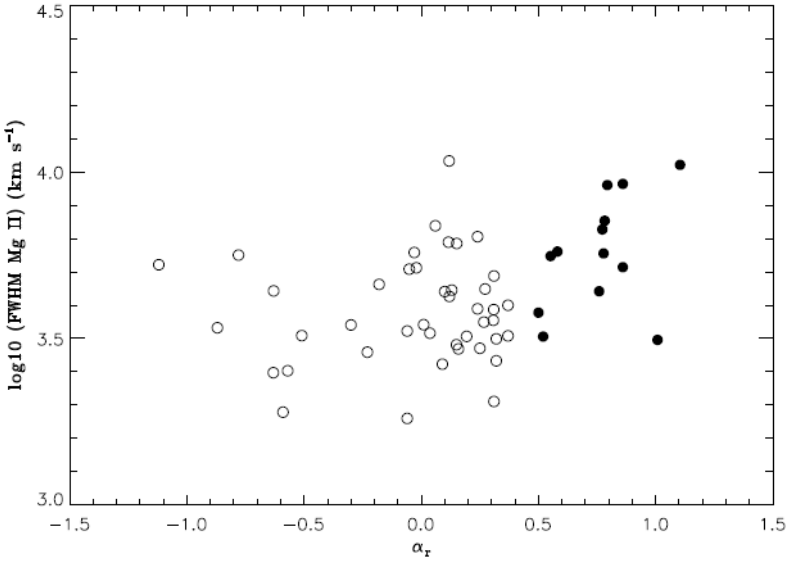

Fig. 5. The line width of broad Mg II line versus radio spectral index. The solid circles represent SSRQs, while the open circles are for FSRQs.

UV/optical variability of SSRQs: change of accretion rate? Gu & Li (submitted to A&A)

- u – i flux-flux diagram for 18 SSRQs
- Standard thin AD with change of accretion rate at constant M_{BH} (Li & Cao 2008)

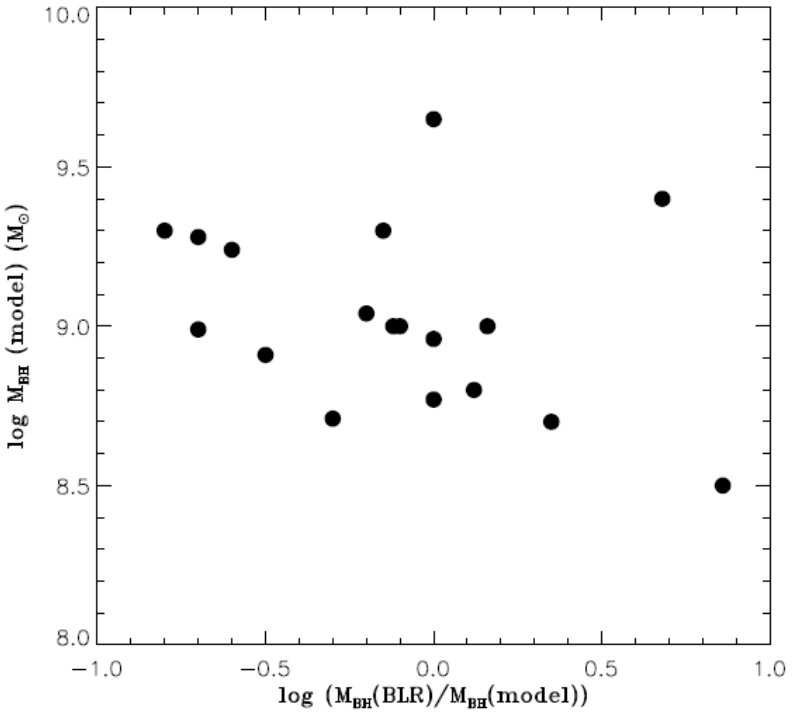

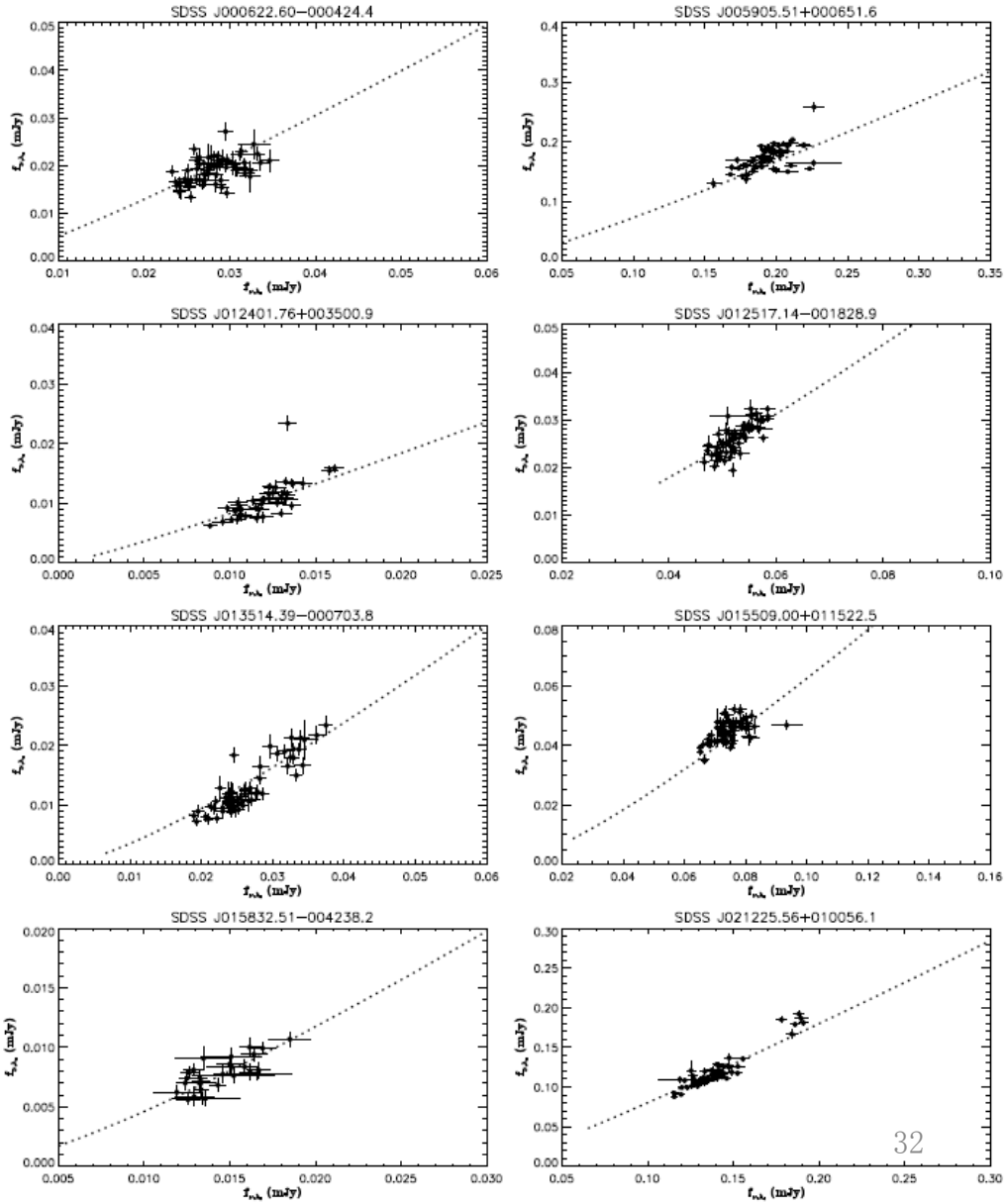

Summary

- Radio-loud quasars all show more or less variations, from 0.18 to 3.46 mag (at r band).
- Redder-when-brighter is rare in FSRQs, which could be explained by the thermal accretion disk emission. In contrast, bluer-when-brighter is more common in FSRQs, and in SSRQs as well.
- The thermal emission from accretion disk may be responsible for the variability in SSRQs, which can likely be caused by the change of accretion rate.
- A disc-like BLR geometry may present in radio-loud quasars.

Thanks for your attention !